Proceedings World Geothermal Congress 2026
Calgary, Canada, June 8 – 11, 2026

Geothermal Performance Forecasting for Optimized Well Placement: Insights and Lessons from Three Case Studies in Indonesia

Ralf Schulze-Riegert[1*], Rindu Intani[2], Fanji Putra[2], Meiyanto Joko Purnomo [2], Sri Mulyani[1], Anugrah Pradana[1], Jean-Pierre Joonnekindt[1], Chris Hug[1]

SLB[1], Star Energy Geothermal[2]

[*]RSchulze-Riegert@slb.com

Keywords: Geothermal reservoir, Fracture characterization, Fracture prediction, Geomechanics, Fracture flow performance, model validation, Make up well placement optimization

ABSTRACT

Techniques for characterizing and modeling fractures in hydrothermal fields are introduced in this paper, aiming to generate fracture models with corresponding permeability distributions for improved reservoir prediction. Natural fracture modeling is guided by key drivers derived from geomechanical principles, which account for stress field perturbations around faults and the effects of pressurized volcanic intrusions and their subsequent cooling. Accurately predicting open and effective fracture densities in data-sparse regions is essential for identifying fracture permeability sweet spots. The reliability of reservoir permeability and connectivity predictions depends on the robustness of these fracture-driving mechanisms. Model validation and uncertainty modeling strategies are introduced to improve model predictability under subsurface uncertainty. Objective measures are defined to quickly validate models against measured data and selecting candidate solutions. Probability maps are generated from multiple realization workflows for robust prediction under subsurface uncertainty. This paper presents three case studies from geothermal reservoirs in Indonesia, highlighting key findings and lessons learned from each.

1 INTRODUCTION

Geothermal reservoirs are key contributors for renewable energy systems and play an important role for electricity generation in Indonesia. Achieving planned increases in energy production through these systems requires a better understanding of driving mechanisms for naturally fractured reservoirs to improve predictability.

Analysis of borehole image logs and Pressure-Temperature-Spinner (PTS) surveys enable detailed characterization of the producing (effective) fractures at the well. The focus on effective fractures associated with the feed zones identified from PTS logs gives a better understanding of the fieldwide distribution and the magnitude of permeability. While this approach targets successful wells in areas with expected higher productivity within the drilled portions of the geothermal reservoir, it misses predictability in undrilled areas for future well pads and make-up wells (Intani et al., 2022).

One aim of this study is to model the 3D fracture distribution calibrated to subsurface well data, in particular, fracture images and production data, and to estimate a permeability distribution to guide infill well locations. Natural fractures can introduce strong anisotropy in geothermal reservoirs that can impact the fluid flow. Therefore, accurate characterization of the fracture network with appropriate ranges in aperture are important at any stage of reservoir management (Joonnekindt, et al., 2022).

The correlation between modeled permeability and measured productivity provides an objective basis for model validation and selection, both well-by-well and on a regional scale. Fracture driver parameterizations are influenced by subsurface uncertainties and significantly affect reservoir flow performance. Consequently, model updates and refinements—guided by validation criteria or new data—are essential. A fully integrated and partially automated workflow enables rapid evaluation of multiple driver scenarios and realizations (Bentley & Smith, 2008) of geometric and aperture-related parameters (Schulze-Riegert, et al., 2022).

This paper presents three case studies from geothermal reservoirs in Indonesia, highlighting key findings and lessons learned from each. It is the first application of this fracture modeling technique to large geothermal projects.

2 GEOLOGICAL BACKGROUND, DATA AND FIELD DESCRIPTION

The geothermal field data used for this comparative study is from three geothermal reservoirs (Darajat, Wayang Windu and Salak) in West Java, Indonesia. All fields are currently operated by Star Energy Geothermal and are briefly described with a focus on geological structures which is the basis for fracture modeling.

2.1 Geothermal fields and description

2.1.1 Darajat

The Darajat geothermal field, located about 230 km southeast of Jakarta, has an installed capacity of 274.5 MWe and is recognized as Indonesia's largest steam-dominated geothermal resource. The Darajat field is located within the larger Kendang volcanic complex, Figure 1, a quaternary volcanic range that includes the active Gunung Papandayan and Gunung Guntur (Rejeki, S., Rohrs, D., Nordquist, G., and Fitriyanto, A., 2010). The geothermal reservoir is within an andesitic-intrusive complex consisting of andesitic lava overlain by pyroclastic breccia that is intruded by diorite and microdioritic dikes and sills (Moore, 2007).

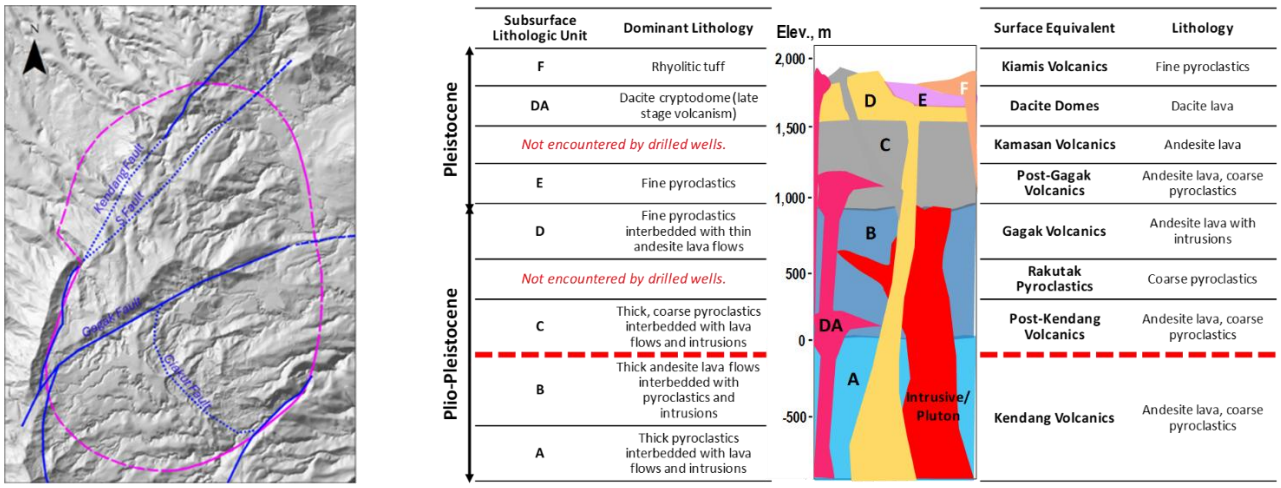


Figure 1 Darajat field showing three main fault systems (left). Schematic geological model of Darajat (right)

Three main faults are identified from the surface and extended into the subsurface. The most western Kendang fault trending nearly north-south with an east dip is interpreted as part of a ring structure of an earlier volcano. The Gagak fault is another prominent surface structure which has most likely formed during the eruption of the resurgent Gagak volcano after the eruption of Kendang, Figure 1. The integration of a provisional reservoir stratigraphy delineated the Ciakut structure, which is a product of a sector collapse inside the Gagak caldera. These surface features are extended into the subsurface and modeled as larger faults that are included in fracture modeling. Shapes and the extent of intrusions are resolved from available geophysical methods and well data. In addition to faults, intrusions are included in fracture modeling as plutons overlain by volcanic strata deposits are forming the reservoir (Hadi, 2001).

2.1.2 Wayang Windu

The Wayang Windu geothermal field, approximately 150 km southeast of Jakarta, has an installed capacity of 230.5 MWe and is a major contributor to Indonesia's geothermal portfolio. The field is a high-terrain geothermal system associated with a series of quaternary volcanoes such as Mount Malabar, Gambung, Bedil, Wayang, and Windu (Mulyadi, Subekti, Pentury, & Azwar, 2023). It is surrounded by high-temperature geothermal fields including the Darajat field. The direction of the structure of Wayang Windu is NNE-SSW in the northern area and NW-SE in the central and south area, with minor N-S. Figure 2.

The lithology of Wayang Windu is divided based on volcanic facies, which can be further categorized into several key lithological units. The rock units encountered in the Wayang Windu field are classified into four facies: Central–Proximal facies consisting of Lava and Breccias, Proximal–Medial facies consisting of Breccias and Tuff Breccias, and Medial–Distal facies consisting of Lapilli and Tuffs, as confirmed by XRF sampling analysis (Masri, Barton, Hartley, & Ramadhan, 2015).

In 2022, the lithological distribution of Wayang Windu was updated, shifting from a facies-based classification to one based on formation distribution Figure 2. This revised approach follows the formation definitions

established by earlier scientific studies, (Ramadhan, Sutrisno, Tasrif, & Bogie, 2012). Chronologically ordered from oldest to youngest: Loka, Waringin, Pangalengan, Dogdog, Malabar, and Wayang Windu.

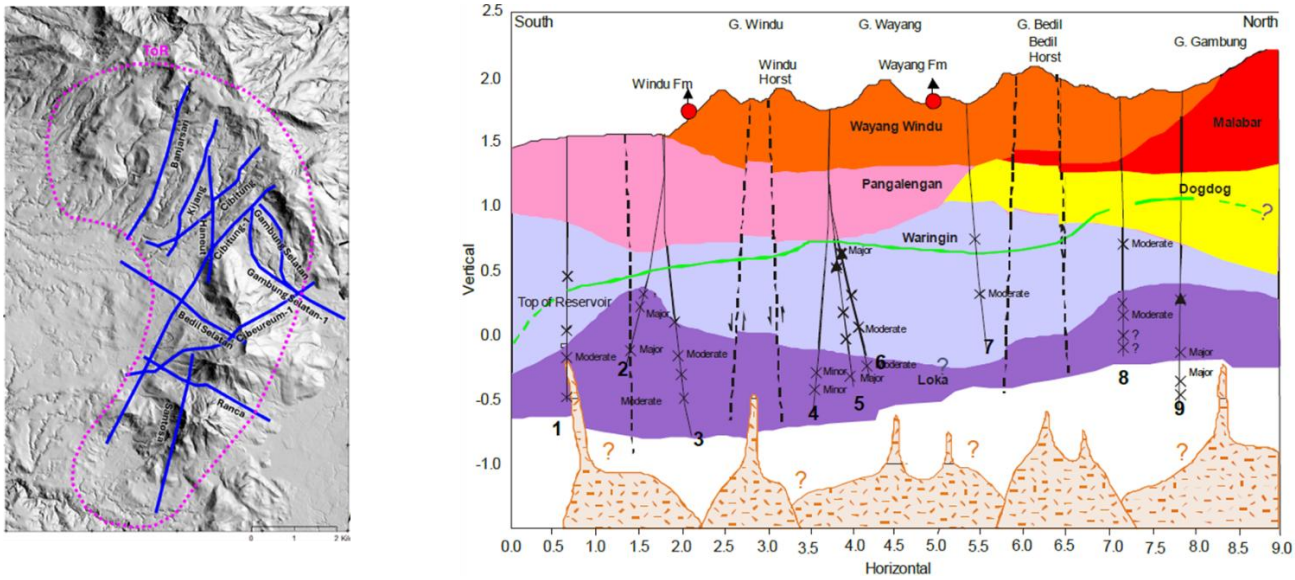


Figure 2 Locations of structures developed in the Wayang Windu area (left). South to North schematic Wayang Windu Geological model (right).

2.1.3 Salak

Salak Geothermal Field, Figure 3, also known as Awibengkok, is situated about 70 km south of Jakarta, has an installed capacity of 397.6 MWe and is Indonesia's largest geothermal producer. The geothermal system lies in a mountain range of inactive andesitic volcanoes, including Mount Salak, Gagak, Perbakti, and Endut, which follow the Sunda Volcanic Arc extending from Sumatra to Flores. These mountains surround the geothermal field and transition into lower hills to the North and South. To the West lies the Cianten Caldera, a collapsed volcanic cone. Structurally, Salak is dominated by a northeast-southwest (NE-SW) trend, which is influenced by the regional stress field of West Java (maximum horizontal stress or SHmax at ~N10°E). This aligns with findings from borehole image logs that show drilling-induced fractures (DTIF) trending north-northeast to south-southwest (NNE-SSW).

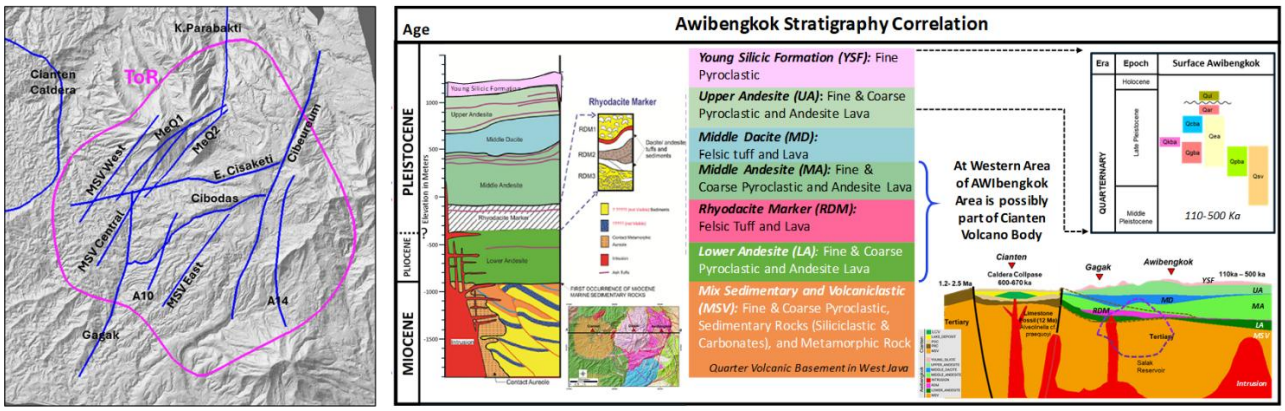


Figure 3 Salak structural map (left). Subsurface stratigraphic section, rock composition and cross section of Awibengkok/Salak Geothermal Field (right).

In terms of stratigraphy, the subsurface rocks at Salak include andesitic and basaltic lava, breccia, tuff, and lahar deposits, formed from long-lived volcanic activity. According to various studies (Stimac et al., 2008; Aprilina et al., 2017), the subsurface rocks are divided into four major formations. From oldest to youngest formations include: (1) Lower volcanic formation that consists of marine sediments and volcaniclastics (MSV) and lower andesite, (2) rhyodacite marker or RDM, (3) middle volcanic formation, and (4) upper volcanic formation. In addition, multiple intrusions are spread all over Salak/Awibengkok geothermal field.

3 GEOLOGICAL MODELING

The interpretation of faults and intrusions define the fundamental geological architecture of the subsurface model impacting the modeled distribution of fractures. The principal method for interpreting fractures is to define drivers, or mechanisms, which constrain fracture orientations and distributions from this subsurface geometry. Assigning apertures and lengths to the discrete fractures modelled from their distributions is the input required to calculate a fracture permeability through the 3D model.

Fracture drivers are the expected controls on fracture distributions and orientations that are modeled either by geomechanical or empirical constraints. The geomechanical drivers work on the principle that fractures develop within a generated perturbed stress field around the fault or intrusion with orientations based on an assigned failure criterion. If regional stress is applied to the interpreted model of the intrusion and faults the stresses will be perturbed by the shape of the structure. Perturbations in stresses in the country rock also result from the pressure inside the intrusion. The rock solid is modeled as a linear elastic material and, therefore standard fracture failure criteria are considered for estimating the fracture orientation of shear or open fractures within the perturbed stress field (Maerten, L., Gillespie, P. and Pollard, D.D., 2002). The distributions of the fractures and their orientations from the empirical driver constraints are based on assigned distributions of fracture intensity away from the fault or intrusion margins into the country rock or intrusion and assigned orientations based on outcrop measurements, log data and process models.

Fracture drivers depend strongly on the structural definition of faults and intrusions. Multiple structural scenarios and multiple realizations of geometric fracture parameter sets add uncertainty to the modeled fracture distributions (Bentley & Smith, 2008). It is the purpose of this work to investigate the impact of permeability distributions on sweet spot analysis and make-up well location selection.

3.1 Structural scenarios

Three structural models were initially selected to accommodate an uncertainty of faults and intrusion shape in the Darajat field (Figure 4). Structural scenario 1 (S1) defines the original intrusion model and fault system (Joonnekindt et al., 2022). A modification of the fault interpretation was done maintaining the intrusion from the S1 scenario for structural scenario 2 (S2). For structural scenario 3 (S3) the original fault interpretation was kept, and a new modified intrusion was used to replace the original intrusion model. This modified intrusion included several narrow plutons rather than a broad low amplitude intrusion as in Scenario 1 and 2.

Structural scenario 1 and 3 have a different 3D structural grid to structural scenario 2 because of the changes to the fault interpretation that requires a different structural framework. Structural scenario 1 also has a different lithology distribution to structural scenario 3, due to the differences in the shape of the intrusion body and overlying section. These combinations make each structural scenario unique in the 3D subsurface shape but also in the modeling grids.

In Salak and Wayang Windu field, one structural model scenario was selected by using the original intrusion and fault model, Figure 4. Uncertainty parameterization for these fields was implemented on a fracture driver level.

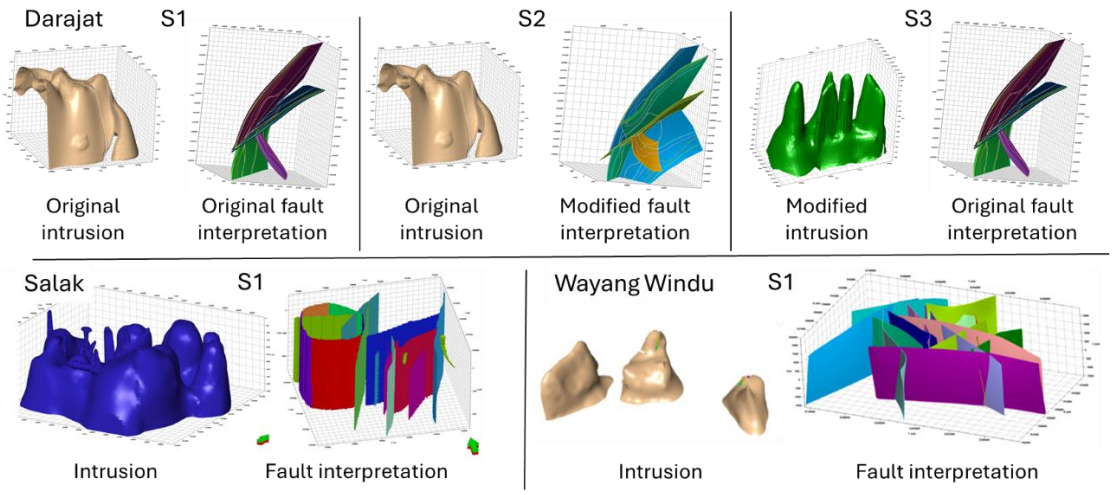


Figure 4 Structural scenarios, Darajat (top), Salak (lower left) & Wayang Windu (lower right)

3.2 Modeling natural fractured systems

3.2.1 Geomechanical and empirical drivers

The geomechanical drivers work on the principle that fractures develop within a generated perturbed stress field around the fault or intrusion with orientations based on an assigned failure criterion. Modeling the rock solid as a linear elastic material has no inherent failure state. In the case of the intrusion driver, it is assumed that the observed natural fractures propagated within a perturbed stress field caused by a deeper, pressurized and more ductile hotter fluid volume intruded into more brittle overlying rocks.

The empirical drivers depend on defined relationships of fracture intensity and orientation around the fault surface or intrusion margin. The intensity away from the fault or intrusion margin is described by a decay law with a decrease in intensity away from the margins. For faults, this is called a damage zone (Kim et al., 2004). The margin distance of fractures in this damage zone may range from 50 to 200 meters but the effective distance is typically much less. This is modelled by decay laws with an exponential drop in fracture intensity close to the fault surface, Figure 5. For Intrusion, this is called thermal cooling effect. The fracture intensity and orientation can be impacted by the drivers described by lateral and vertical changes caused by thermal cooling of volcanic intrusion in the host rock and the intrusion body.

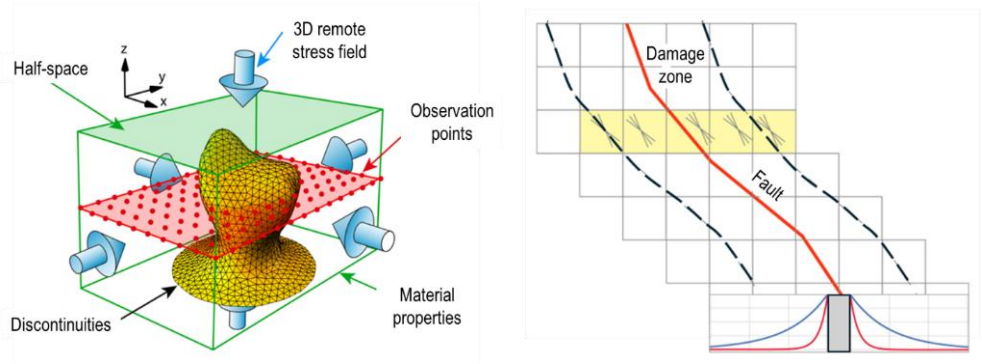


Figure 5 Stresses perturbed in country rock from intrusion pressure and around intrusion shape from regional far-field stress, left. Fracture damage zone around a principal fault surface and an example for decay laws for the distance to fault intensity, right.

3.2.2 Calibrating fracture intensity

The fracture drivers define areas of higher or lower expected fracture intensity. In the case of geomechanical drivers, we might expect a greater number of fractures in areas with higher stress concentration. For empirical drivers the intensity is defined and decreases away from the fault or intrusion margin. Comparing the fracture intensity from the modeled drivers to the image log data along the well paths provides an intensity calibration and a validation of the driver's ability to consume the fractures in the wells.

A key constraint is to determine which fractures imaged in the wells are related to a given driver. The method applied here is to define a tectonic order to the deformation by driver, and for each tectonic event determine which of the fractures from the wells are "consumed" by that driver and remove those fractures as unavailable for the subsequent tectonic event associated with a driver. The consumed fractures for a particular driver are available for calibration of the intensity. This process comes with some risks particularly for empirical drivers as it is possible that the wells do not penetrate the prescribed distance from the margin or within the fault damage zone. This is less of an issue in geomechanical models as the stresses are distributed across the entire model.

3.2.3 Discrete fracture network creation and upscaling

The discrete fracture network (DFN) is used to obtain a continuum approximation of reservoir fracture system properties, equivalent fracture porosity and permeability, as well as exchange mass factor (sigma) between matrix and fractures. The combination of the fracture intensity, dip angle and dip azimuth from the drivers is modeled with a range of fracture length and aperture to create the fracture reservoir properties after upscaling. Changes in the distribution and orientations of both fracture length and aperture will affect the fracture property distribution as well as their absolute values. The aperture and length selection in the models is an automated process allowing multiple realization model results from a distribution in properties. The results from the upscaled permeability from the different models of fracture distributions are provided as input for a sensitivity analysis as compared to the production data (Schulze-Riegert, et al., 2022). This analysis is described in the next section.

4 UNCERTAINTY MODELING AND MODEL VALIDATION

Subsurface uncertainty in this study is represented by multiple structural models and variations of driver contributions explaining observed fractures. Aperture and fracture length have a high impact on permeability upscaling and are validated against measured permeability from well performance analysis.

Multiple realization results depend on modifying fracture geometry and aperture parameters in the discrete fracture creation process. The process is repeated for different structural scenarios and alternative fracture driver sets. This generates a high number of discrete fracture network models which cannot be validated by visual inspection. Performance measures are defined to validate models on a regional level for which permeability data is available (Schulze-Riegert, et al., 2022).

4.1 Model validation

Models are validated by comparing upscaled permeability distributions from fracture models to measured permeability data from wells in selected regions. In case of the Darajat model, measurement data is available for 8 regional volumes which are represented by delineated areas in Figure 6.

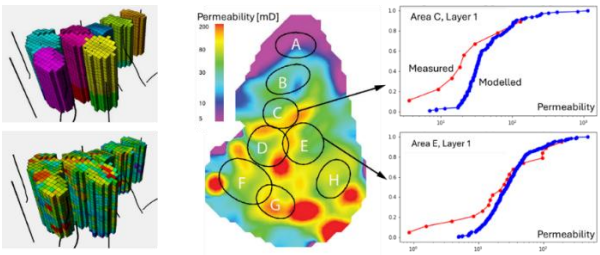


Figure 6 Modeling volumes (upper left) and permeability distribution in the same volumes (lower left). Delineated areas with available measurement data (middle). Comparison of measured (red) to modelled (blue) permeability distributions for two selected areas (right).

Q_{mean} is defined as a measure for the difference between the geometric mean of modelled and measured permeability data, Eq.(1). It is normalized by a tolerance level or statistical error σ_{err}. For each selected volume the objective measure for the mismatch between measured and modelled permeability is calculated.

$$Q_{mean} = \left| \frac{k_{mean} - k_{mean}^{ref}}{\sigma_{err}} \right| \tag{1}$$

k_{mean} of modelled and k_{mean}^{ref} of measured reference permeability data is calculated as the geometric mean and the error term σ_{err} is calculated as an estimated standard error of the mean. A model is acceptable if the mismatch is of the order of the tolerance-level, i.e., $Q_{mean} \sim 1$. Permeability contrasts are captured by the ratio between different regional permeability distributions and can be directly compared to the corresponding ratio of measured data, Eq.(2).

$$R = \frac{k_{mean}^{Area\ A}}{k_{mean}^{Area\ B}} \tag{2}$$

4.2 Result analysis: Multiple scenario - multiple realization workflow

An execution design including structural models, fracture drivers and DFN setting is shown in Figure 7, left. The diagram represents a hierarchy of modeling steps, i.e., structural scenarios (top), order of four driver contributions (middle), discrete fracture network modeling and upscaling to permeability distributions (bottom). On each horizontal level green circles represent variations of individual driver contributions, e.g., intrusion, thermal cooling, distance to fault and natural fracture prediction away from principal fault surfaces. For the given example the red line connects 6 nodes of modeling contributions for the final DFN model including variations in fracture length and aperture.

Testing all possible combinations for each driver parameter requires significant modeling and computational effort. Taking the example of the Darajat field, discrete parameter sets were selected within predefined ranges for each driver that explain the greatest number of fractures over others. For each structural scenario five distinct driver sets were selected to represent uncertainty. Figure 7 (middle) shows the absolute permeability mismatch Eq.(1) and the ratio of permeability Eq.(2) as a function of mean aperture.

The black dashed line defines a threshold for the mismatch calculation. Models below the line are acceptable, which applies for a subset of model scenarios and realizations. Both objective measures give a fast overview of model performance and define efficient selection criteria.

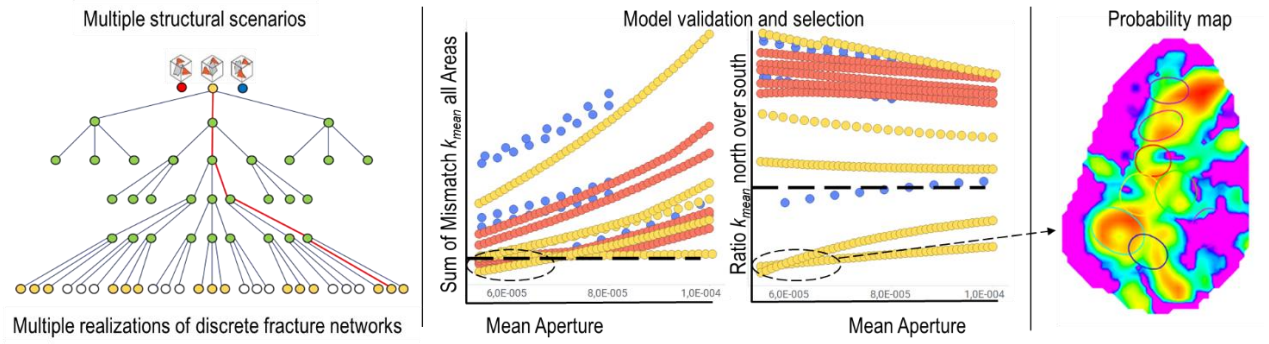


Figure 7 Combinations of discrete structural scenarios and fracture drivers sets as an input to multiple realizations of discrete fracture networks (left) . The top level represents 3 structural scenarios (red, yellow, blue) followed by 4 levels of driver realizations (green). The lowest level represents DFN realizations with selected driver combinations shown in yellow. Model validation results are shown for 5 driver sets for each structural scenario (red, yellow, blue) as a function of mean aperture, shown for the absolute match (middle) and the ratio (right). A selection of multiple realization DFNs are input to probability maps (right).

4.2.1 Sweet spot analysis under uncertainty

An ensemble of multiple realizations within acceptance criteria represents subsurface uncertainty. Robust well location selection needs to account for subsurface uncertainty beyond a single deterministic model. Probability maps in this work are defined to capture uncertainty with respect to economic threshold criteria. The decision (recommendation) for well placement locations is linked to a probabilistic criterion which prepares a Yes/No outcome. Probability maps are calculated to give the probability of finding areas with permeability larger than a project related threshold, e.g. 30 mD. A decision criterion could state a minimum 90% probability for permeability being over 30 mD in an area of interest. In Figure 7 (right) this applies to areas with a warm red color.

5 APPLICATION

The workflow design applied to all three fields is captured in Figure 8. Fracture characterization, structural modeling building and fracture driver creation builds on manual modeling and analysis steps for the setup of multiple scenarios (Joonnekindt, et al., 2022). Variations of fracture geometry and aperture in the discrete fracture network creation are fully automatized and allow generating multiple realizations for comparison to measured data. Automatically exported permeability data (Petrel, 2024) consitute a data base for model validation, analytics and selection of representative cases (Schulze-Riegert, et al., 2022).

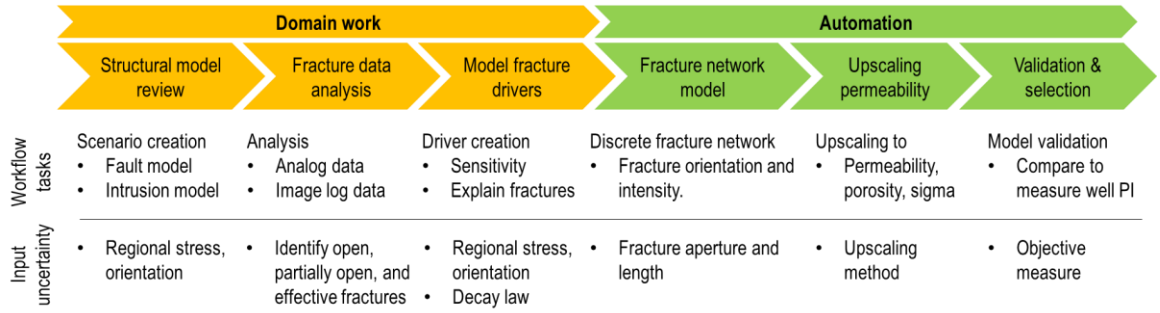


Figure 8 Generic workflow design including work steps and input uncertainty. The domain work is dominated by manual work steps (left); a multiple DFN realization workflow and model validation are automated (right).

5.1 Darajat

Out of 30 wells that have borehole image logs at Darajat, 18 wells were chosen for this study based on their location. High confidence open, partially open, and effective fractures (based on PTS logs) have been interpreted from image logs. Open fractures with an expected potential to add to production were identified and included in the fracture modeling process. The methodology and workflow design described in this work has been used to model the distribution of fractures in the Darajat reservoir field. Four fracture driver systems were included; for

fractures related to pressurized emplacement of igneous intrusion(s) into the host rocks within and below the geothermal system, for fractures caused by thermal expansion and contraction of the intrusion(s) and host rocks, for fractures within a damage zone around faults and for the fractures that result from stress perturbations throughout the reservoir rock volume at the bends, intersection, and tips of interpreted faults (Maerten, L., Gillespie, P. and Pollard, D.D., 2002). Multiple structural scenarios and DFN realizations have been created, following the conceptual workflow Figure 8. Model validation criteria were applied to select structural scenarios and related multiple realizations of DFNs, Figure 7. Probability maps with economic threshold criteria were generated for robust sweet spot identification shown in Figure 9.

Fieldwide trends of fracture permeability derived from the DFNs were compared to those from the Darajat numerical model. Trends of high permeability in delineated areas including existing production wells in the upscaled DFN models resulted in trends that are similar to those found in the Darajat numerical model. Trends show two key features; high permeability hot spots in the North and South and a connection, but of lower permeability through the central field, (Intani et al., 2022).

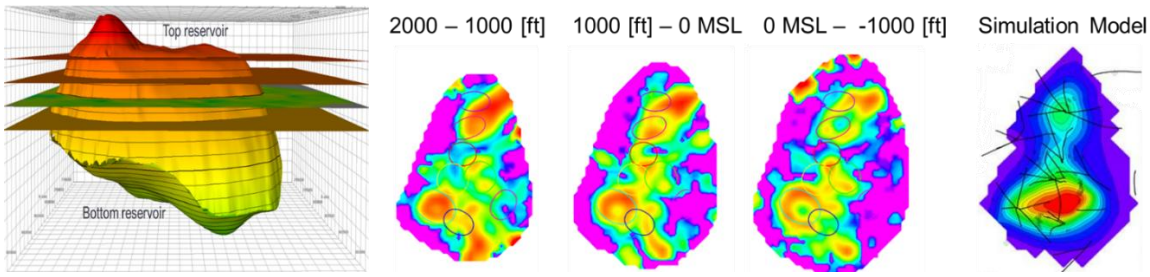


Figure 9 Reservoir model with 3 depth zones (left) and probability maps (right). Red warm color indicates a high chance for permeability above a minimum economic operating condition for hydrothermal production wells.

Probabilistic permeability maps were used to identify sweet spots in areas with no available measurement data for model validation. In parallel, dynamic models were used to guide well placement. The alignment between both result interpretations and the success of recent drilling campaigns has increased confidence in the decision process on well placement where both static and dynamic modeling plays an important role.

5.2 Wayang Windu

One structural scenario was created for modeling Wayang Windu reservoir. Only minor revisions in the intrusion and fault model were added after insights from the model validation process were available. The fracture characterization and modeling workflow described in this work (Figure 8) successfully explained observed fracture data. In the final model, structure, intrusion geobody, geomechanical stress fields around faults explained more that 90% of observed fractures, more than for any other geothermal reservoir described in this paper. The geological model was validated based on two reservoir zones described in Figure 10. For each delineated area, the distribution of upscaled permeability values was compared to the formation zone distribution in correlation with productivity index (PI) values.

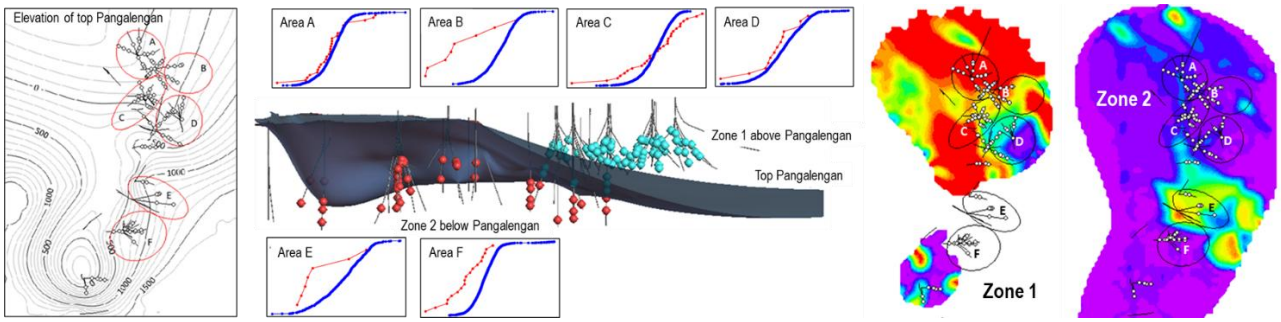


Figure 10 Well location map (left). Measured (red) vs. modelled permeability distribution in delineated areas in zone 1 (top) and zone 2 (bottom). Zone 1 and zone 2 probability maps (right).

Zone 1 represents the steam cap reservoir in the North and shows a high probability of permeability (PoP) above an economical threshold extended to the NW area of Wayang Windu. Zone-2 represents the liquid reservoir in the central area and shows high PoP to the SE of the drilled area, Figure 10. The Wayang Windu team developed a well plan for 2026 make up wells by utilizing geological and probabilistic modeling results described here as one of the considerations for sweet spot area targets.

5.3 Salak

Two structural scenarios were created for the Salak static reservoir model. Following the workflow in Figure 8 the resulting fracture permeability model was first validated against measured permeability in all delineated well areas. The strong contrast between measured high and low permeability areas could initially not be reproduced by the upscaled permeability model. Measured permeability in areas F and H was significantly higher compared to other areas B, I and G, Figure 11.

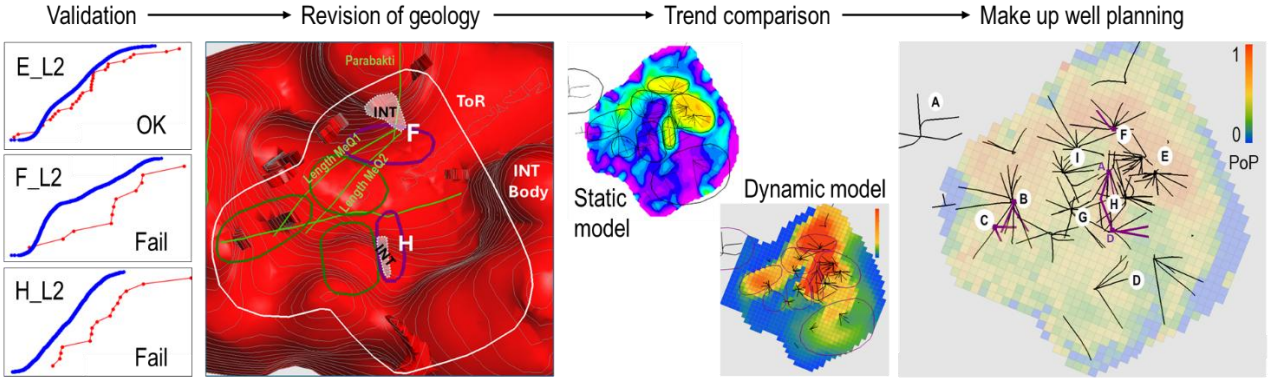


Figure 11 Model validation followed by a revision of the geology scenario, comparison of static and dynamic permeability trends and make up well planning for Salak reservoir in selected sweet spot areas.

A second structural scenario was developed, motivated by insights from the model validation of scenario 1. Higher permeability contrast in the field was supported by selected geological modifications of the model. In area (F) the Parabakti fault was added to the model with a SE dipping. Additional changes included extending faults (MeQ1 and MeQ2) to the Parabakti structure, introducing an intersection to the Kawah Parabakti fumarole and a fault surface starting in middle Andesite surface. Based on well and gravity data a small intrusion was added near the Kawah Parabakti fumarole structure and central area to support a requirement for an increase of permeability in area F and H. In addition, a dip was implemented for the fault systems East Cisaketi and Cibodas to support a higher permeability in area H. Lower permeability in areas B, G and I was achieved by modifying input to the natural fracture prediction for faults with impact on those areas. The revised geological model predicted similar permeability trends in areas of existing wells compared to the dynamic model and was one input to the sweet spot area analysis used for the Salak make up well planning 2025-2026, Figure 11.

CONCLUSION

This work has applied geomechanical and empirical fracture driver systems to explain observed fractures in image log data. Geomechanical techniques are an established practice for modeling naturally fractured hydrocarbon reservoir systems. The application to geothermal systems in a volcanic context is novel, in particular, geomechanical fracture driver systems describing pressurized emplacement of igneous intrusion into the host rocks within and below the geothermal system. Structural models, sets of fracture driver systems and multiple realizations of discrete fracture networks were created and validated against measured well data.

The workflow was initially developed for the Darajat geothermal field in close cooperation between Star Energy Geothermal and SLB. In three consecutive project phases over a 3-year period the technology was (1) benchmarked, (2) extended to uncertainty modeling and (3) transferred to the asset teams for independent project execution. The strong domain expertise of Start Energy Geothermal along with the technology delivery and development by SLB has significantly strengthened the integrated team productivity to successfully deliver results. An international team with experts working across 12 time zones was a benefit to collect expertise and a challenge for finding acceptable time windows for synchronization in phase 1 and 2. Local teams in phase 3 covered most support and benefited from standard working times.

The fracture characterization and optimizing well production project "enhanced understanding of effective permeability distribution in the field: We have developed the world's first fracture characterization map and continuously update the model with the latest drilling results to improve well placement accuracy and avoid non-productive drilling targets", CEO of Star Energy Geothermal, (Tan, 2025).

Future work needs to focus on the integration between static and dynamic modeling. Static models need to be benchmarked on heterogeneity and connectivity to provide a direct input to the dynamic model (Schulze-Riegert et al., 2024). The dynamic model is validated on production data and delivers feedback on the performance of

the static model. Model validation and maturation should follow an integrated closed loop between static and dynamic models to improve predictability under subsurface uncertainty and to shorten decision cycles with higher confidence.

Acknowledgements

The authors of this paper would like to thank the management of Star Energy Geothermal and SLB for supporting this work. Conclusions and opinions stated in this paper are those of the authors and do not necessarily represent those of Star Energy Geothermal or SLB. The authors also like to recognize Russell Davies for his expertise and contributions to the project.

REFERENCES

Bentley, M., & Smith, S. (2008). Scenario-based reservoir modelling: The need for more determinism and less anchoring. *Geological Society*, 145-159. doi:10.1144/SP309.11

Hadi, J. (2001). The Darajat Geothermal Field Conceptual Model, A Vapor-dominated System. Yogyakarta, Indonesia: 5th INAGA Annual Scientific Conference and Exhibition.

Intani et al., R. (2022). Pioneering the use of natural fracture modeling for well placement at Darajat Field, Indonesia. *Workshop on Geothermal Reservoir Engineering*. Stanford University.

Joonnekindt, J. P., Diaz, F., Davies, R., Hultzsch, P., Mulyani, S., Intani, R., . . . Gunderson, R. (2022). Innovative Technical Strategies in Natural Fracture Characterization for Well Placement: Case Study from Darajat Field, Indonesia. International Petroleum Technology Conference. doi:10.2523/IPTC-22373-MS

Maerten, L., Gillespie, P. and Pollard, D.D. (2002). Effects of local stress perturbation on secondary fault development. *Journal of Structural Geology, 24*(1), 145-153.

Masri, A., Barton, C., Hartley, L., & Ramadhan, Y. (2015). Structural Permeability Assessment Using Geological Structural Model Integrated with 3D Geomechanical Study and Discrete Facture Network Model in Wayang Windu Geothermal Field, West Java, Indonesia. *Fourtieth Workshop on Geothermal Reservoir Engineering*. Stanford Geothermal Program.

Moore, J. (2007). *The Hydrothermal Evolution of the Darajat Geothermal System, West Java, Indonesia*. Unpublished Technical Report Prepared for Star Energy Geothermal.

Mulyadi, Subekti, D., Pentury, S., & Azwar, L. S. (2023). Responses of Wayang Windu Geothermal Reservoir to Over 20 Years of Production. *World Geothermal Congress* .

Petrel. (2024). *Subsurface Software*. SLB.

Ramadhan, Y., Sutrisno, L., Tasrif, A., & Bogie, I. (2012). Geological Evaluation of the Waringin Formation as the host of a Vapor-Dominated Geothermal Reservoir at the Wayang Windu Geothermal Field. *New Zealand Geothermal Workshop*.

Rejeki, S., Rohrs, D., Nordquist, G., and Fitriyanto, A. (2010). Geologic Conceptual Model Update of the Darajat Geothermal Field, Indonesia. Bali, Indonesia: World Geothermal Congress.

Schulze-Riegert, R., Davies, R., Coronado, J., Hug, C., Joonnekindt, J., Mulyani, S., . . . Putra, F. (2022). Well Placement Optimization for Geothermal Reservoir Under Subsurface Uncertainty. *ECMOR 2022*. EAGE. doi:10.3997/2214-4609.202244094

Schulze-Riegert, R., Natvig, J., & Marquez, D. (2024). Geological Screening of Models with Different Grid Types using Multiscale Reservoir Simulation. *ECMOR 2024*. EAGE. doi:10.3997/2214-4609.202437102

Tan, H. S. (2025). Driving Innovation in Geothermal Operations: Lessons from the Field. *Geothermal Convention & Exhibition 17-19.Sep. 2025*. Jakarta, Indonesia.